Squaraines: Crystal Structures and Spectroscopic Analysis of Hydrated and Anhydrous Forms of Squaric Acid–Isoniazid Species

ARTICLE *in* THE JOURNAL OF PHYSICAL CHEMISTRY A · DECEMBER 2014

Impact Factor: 2.69 · DOI: 10.1021/jp509502w · Source: PubMed

5 AUTHORS, INCLUDING:

Luiz Fernando Cappa De Oliveira

Federal University of Juiz de Fora

175 PUBLICATIONS **1,759** CITATIONS

SEE PROFILE

THE JOURNAL OF PHYSICAL CHEMISTRY A

Article

pubs.acs.org/JPCA

Squaraines: Crystal Structures and Spectroscopic Analysis of Hydrated and Anhydrous Forms of Squaric Acid-Isoniazid Species

Felipe D. dos Reis,[†] Isabela C. Gatti,[†] Humberto C. Garcia,[†] Vanessa E. de Oliveira,[‡] and Luiz F. C. de Oliveira*,[†]

[†]Núcleo de Espectroscopia e Estrutura Molecular (NEEM), Departamento de Química, Instituto de Ciências Exatas, Universidade Federal de Juiz de Fora, Juiz de Fora, MG 36036-900, Brazil

[‡]Instituto de Ciência e Tecnologia, Universidade Federal Fluminense, Rio das Ostras, RJ 28890-000, Brazil

Supporting Information

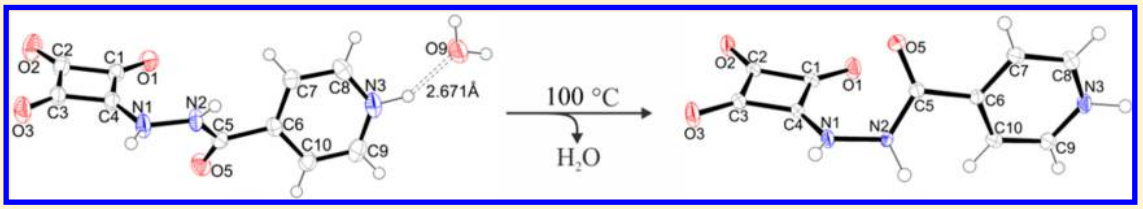

ABSTRACT: The crystal structures, synthesis procedure, thermal behavior, and spectroscopic properties of a new squaraine SqINH·H_2O and its anhydrous arrangement are described. This squaraine is obtained through an acid−base reaction using squaric acid (H_2Sq) and isoniazid (INH) as precursors. Both squaraines crystallize in the monoclinic system, but in different space groups: the hydrated and anhydrous arrangement crystallizes in the $P2_1$ and $P2_1/c$ space group, respectively. The crystallographic data strongly suggest that the structures present an expressive increase in their electronic delocalization all over the molecular structure of both compounds, when compared with the reagents. The bond distances for both structures present an average value intermediate between a single and double character (1.463(3) Å for SqINH·H_2O and 1.4959(3) Å for SqINH). The vibrational and electronic data also corroborate with this proposal, since the band shifts indicate that the conjugation over the system is increased, as indicated by the blue shift observed for the carbonyl stretching bands for both compounds. The presence of the water molecule is responsible for a decrease in fluorescence emission, as determined by the emission spectra recorded for both compounds.

INTRODUCTION

Oxocarbons are an important class of anionic molecules formed by "*n*" carbon and oxygen atoms with general formula $(C_nO_n)^{2-}$, where "*n*" varies from 3 to 6 for deltate, squarate, croconate, and rhodizonate, respectively.[1,2] Such systems possess interesting structural features such as flat cyclic structures, high molecular symmetry (D_{nh}) and an extensive π electron delocalization.[2−4] The partial or total substitution of the oxygen atoms by other groups originates systems named pseudo-oxocarbons,[5,6] and the oxygen(s) substitution(s) in the squaric acid (H_2Sq, $n = 4$) by nitrogenous groups engenders the so-called squaraines,[5,7] see Figure 1a.

Squaraines are a very special class of organic dyes with countless chemical and physical applications, such as metal detection,[8−10] photodynamic therapy (PDT),[11] dye-sensitized solar cells,[12,13] and photothermic therapy.[14,15] Squaraines are formed by a four-membered ring with notably electronic deficiencies besides the presence of the two electron-donating groups.[16] Most of these systems are photostable molecules with a very useful property of light absorber in the visible and infrared regions of the electromagnetic spectrum.[3,17−19] In general, squaraines are obtained by the reaction between H_2Sq and a nitrogenous compound, by nucleophilic substitution of at least one of the oxygen atoms from the oxocarbon ring by a compound or group with expressive electronic delocalization. In the present work, the nitrogenous system used is isoniazid (INH), whose structure is shown in Figure 1b. INH is widely used as a prescription for tuberculosis treatment, and it is proven to be efficient against this contagious bacterial infection caused by the *Mycobacterium tuberculosis* complex.[20] In the past few years, tuberculosis has been one of the five diseases that causes a greater amount of mortality in human beings in underdeveloped countries.[21] INH hydrolyzes with time and inappropriate storage conditions, resulting in the hydrazine formation. Hydrazine is known to be toxic and carcinogenic and, due to this, INH has been reported to be carcinogenic in mice;[22] this is why INH quantitative analysis in pharmaceutical preparations and biological fluids are important issues that involve public health. In this context, Naik et al. described a new method for the quantification of INH using a ligand substitution kinetic assay.[23] That study proposed the interaction of INH with $[Fe(CN)_5(H_2O)]^{3-}$ in aqueous solution and the analysis of the product by spectrophotometric methods.

Received: September 19, 2014
Revised: November 22, 2014

   dx.doi.org/10.1021/jp509502w | *J. Phys. Chem. A* XXXX, XXX, XXX−XXX

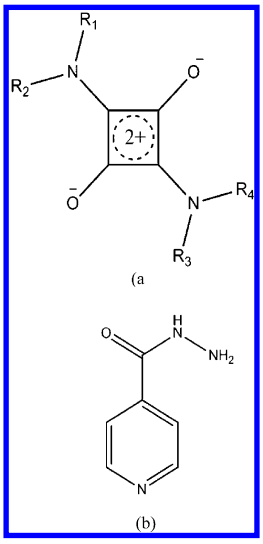

Figure 1. Molecular formula of a general squaraine (a) and isoniazid (b).

Interest in INH derivatives has been increasing over recent years; some INH-derived species are more active against the aforementioned bacteria than INH individually.[24] Imramovský et al. describes the synthesis of several of these derivatives. The vast majority of these compounds has a heterocyclic structure containing oxygen and nitrogen atoms presenting higher lipophilicity than INH, which means that such molecules are more effectively transported through the cellular membranes. This enhanced property makes some of the derivatives more effective against bacteria.[25] Shingnapurkar et al. proposed some pyruvate-isoniazid conjugates and some copper complexes; their results showed remarkable antitubercular activities.[26] However, neither of these works presents a detailed study for this class of molecules from a spectroscopic point of view, which is the focus of this present work.

Recent studies show that squaraine dyes have a very important application as a light absorber and fluorescent chemosensor. It was shown that the increase of polarity and conjugation degree of the groups attached to the oxocarbon ring make squaraines more efficient in converting solar light to electricity.[27] In another study, the squaraine–bis(rhodamine-6G) was proven to be highly efficient in the detection of Hg^{2+} ion in acetonitrile solution.[28] It was observed that the squaraine coordinates to the metal ion as a tridentate ligand.

In this work, we present the synthesis and the spectroscopic characterization of the squaraine obtained from the reaction between squaric acid and INH. The results concerning the crystal structures and the supramolecular arrangements, based on intermolecular interactions, are discussed together with the spectroscopic properties, trying to correlate the crystalline structure for both compounds, and the electronic and vibrational characteristics.

EXPERIMENTAL SECTION

Chemicals and Reagents. Isonicotinic hydrazide (isoniazid, INH) and squaric acid (H_2Sq) were both purchased from Sigma-Aldrich and used as received without further purification.

Synthesis of [((4-Hydrazinecarbonyl)pyridine)-squarate] Hydrated (SqINH·H_2O). In a beaker was heated at 50 °C for 1 h a mixture of isoniazid (0.15 g, 1.09 mmol), solubilized in 10 mL of distillated water, and squaric acid (0.25 g, 2.19 mmol), solubilized in 15 mL of distillated water. A yellow precipitated was filtered, and the resultant solution was kept reserved for 3 days; orange crystals were obtained by slow solvent evaporation. Yield: 9.8%. Elemental analysis of $C_{10}H_9N_3O_5$ (251.20 g mol^{-1}) gave the following data (%). Calculated: C, 47.81; H, 3.61; N, 16.73. Found: C, 46.81; H, 3.60; N, 15.45.

Synthesis of [((4-Hydrazinecarbonyl)pyridine)-squarate] (SqINH). Crystals of the nonhydrated compound (SqINH) were obtained from SqINH·H_2O, after heating at 100 °C for 3 h in a heater that kept the temperature constant.

Instrumentation. Thermogravimetric (TG) and differential thermal analyses (DTA) were performed using a Schimadzu TA-60 WS, with a DSC-60 calorimeter and a DTG-60 thermogravimetric system. The curves were accomplished at a rate of 10 °C/min from 25 to 900 °C in a nitrogen atmosphere.

Raman spectra were measured from the solid phase, using a Bruker RFS 100 instrument and an Nd^{3+}/YAG laser operating at 1064 nm with a 4 cm^{-1} spectral resolution, equipped with a Ge detector cooled with liquid nitrogen. Raman spectra in the visible region were obtained from a Bruker SENTERRA spectrometer with a green laser operating at 532 nm, equipped with a CCD detector. All the spectra were obtained at least twice to guarantee reproducibility of bands intensity and position. Infrared (IR) spectra were recorded in an Alpha Bruker FT-IR spectrometer, in the region of 360–3500 cm^{-1}, with the sample supported at the KBr pellet, with 4 cm^{-1} of spectral resolution, and average of 128 scans. The electronic spectra were obtained in a Shimadzu UVPC 1601 spectrophotometer using 10.0 mm quartz cell, in the region of 190 to 1100 cm^{-1}.

Single crystal X-ray data were collected using an Oxford GEMINI A Ultra diffractometer with Mo Kα (λ = 0.71073 Å) at room temperature (150 K). Data collection, reduction, and cell refinement were performed by CrysAlis RED, Oxford Diffraction Ltd., version 1.171.32.38 program.[29] An empirical isotropic extinction parameter x was performed, according to the method described by Larson.[30] A multiscan absorption correction was applied.[31] The structures were drawn by ORTEP-3 for Windows[32] and Mercury[33] programs. Hydrogen atoms were located from Fourier difference maps. Anisotropic displacement parameters were assigned to all non-hydrogen atoms. CCDC number 947594 and number 970621 contain the supplementary crystallographic data for these compounds. These data can be obtained free of charge at www.ccdc.cam.ac.uk/conts/retrieving.html or from the Cambridge Crystallographic Data Centre, 12 Union Road, Cambridge CB2 1EZ, UK [Fax (internat.), 1 44–1223/336–033; e-mail, deposit@ccdc.cam.ac.uk].

RESULTS AND DISCUSSIONS

The thermogravimetric analyses were performed for SqINH·H_2O and SqINH compounds in nitrogen atmosphere; the respective curves can be found in the Supporting Information. Those data show the absence of solvent molecules in SqINH and the presence of one water molecule in SqINH·H_2O. The curve for SqINH·H_2O shows a weight loss at 75 °C related to the loss of one noncoordinated water molecule (calc/expt 7.17/7.31%). The DTA shows that the water molecule loss is an endothermic event. The thermal behavior of SqINH is very similar to the hydrated compound after 115 °C, where it can be seen that the TG curves do not show any weight loss until 250

dx.doi.org/10.1021/jp509502w | J. Phys. Chem. A XXXX, XXX, XXX–XXX

°C. Above this temperature occurs the thermal decomposition for both compounds, which are exothermic events. No residual materials were observed at the end of the respective analysis.

Crystal data of SqINH·H_2O and SqINH are listed in Table 1; the main geometrical parameters are shown in Tables 2 and 3,

Table 1. Crystallographic Data of the Squaraines SqINH·H_2O and SqINH

	SqINH·H_2O	SqINH
formula	$C_{10}H_9N_3O_5$	$C_{10}H_7N_3O_4$
formula weight/g mol^{-1}	251.20	233.19
temp./K	298(2)	150
crystal system	monoclinic	monoclinic
space group	$P2_1$	$P2_1/c$
a/Å	5.1063(3)	4.7174(2)
b/Å	8.2192(5)	9.7934(6)
c/Å	12.3887(7)	21.0604(13)
α	90.00	90.00
β	100.425(5)	90.872(5)
γ	90.00	90.00
V/Å^3	511.37(5)	972.87
Z	2	4
crystal size/mm^3	0.09 × 0.157 × 0.636	0.41 × 0.24 × 0.18
D_{calc}/g cm^{-3}	1.631	0.24
μ(Mo Kα)/cm^{-1}	0.134	0.18
transmission factors (min/max)	0.975/0.987	0.964/0.977
reflections measured/unique	8357/2110	16437/1981
observed reflections [$F_o^2 > 2\sigma(F_o^2)$]	1924	1532
no. of parameters refined	184	166
$R[F_o > 2\sigma(F_o)]$	0.0330	0.0544
$wR[F_o^2 > 2\sigma(F_o)^2]$	0.0738	0.1366
S	1.062	1.072
RMS peak	0.038	0.083

whereas the crystal structures can be seen in Figure 2, which exhibits the repeating unit of the two-monosubstituted pseudo-oxocarbons obtained through the condensation reaction

Table 2. Main Geometric Parameters of the Squaraines SqINH·H_2O and SqINH

	SqINH·H_2O	SqINH
	Bond Distance/Å	
O5−C5	1.225(2)	1.228(3)
N2−C5	1.335(2)	1.350(3)
N2−N1	1.390(2)	1.397(3)
N3−C8	1.333(3)	1.337(3)
O1−C1	1.243(2)	1.236(3)
O2−C2	1.226(2)	1.248(3)
O3−C3	1.242(2)	1.253(3)
N1−C4	1.335(2)	1.325(3)
C1−C4	1.438(3)	1.464(3)
C1−C2	1.495(3)	1.476(3)
C4−C3	1.433(3)	1.440(3)
C3−C2	1.485(2)	1.474(3)
	Average of Bond Angles/deg	
C4− C1 −C2	88.74(14)	88.27(17)
C3− C4 −C1	93.15(15)	92.16(17)
C4−C3 −C2	89.31(14)	89.24(17)
C3−C2−C1	88.80(14)	90.31(17)

Table 3. Hydrogen Bonds Lengths of the Squaraines SqINH·H_2O and SqINH

SqINH·H_2O		SqINH	
D−H···A/Å		D−H···A/Å	
N2−HN2···O1	2.771(2)	N2−HN2···O5	2.835(2)
N3−HN3···O9	2.671(3)	N1−HN1···O3	2.694(3)
N1−HN1···O5	2.881(2)	N3−HN3···O2	2.625(2)
O9−H9A···O2	2.761(2)	C7−H7···O1	3.146(3)
O9−H9C···O3	2.710(2)		
D−H···A/deg		D−H···A/deg	
N2−HN2···O1	156.3(19)	N2−HN2···O5	150(3)
N3−HN3···O9	150(2)	N1−HN1···O3	171(3)
N1−HN1···O5	168(2)	N3−HN3···O2	169(3)

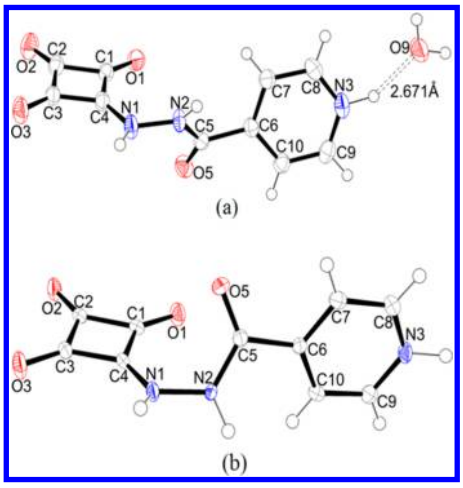

Figure 2. Asymmetric unit of the squaraines SqINH·H_2O (a) and SqINH (b).

between squaric acid and isoniazid. It occurs through the loss of the −OH group from the squaric acid and entrance of the INH molecule through its -NH_2 group with release of one water molecule. The complete neutralization of the oxocarbon dianion occurs by protonation of the nitrogen atom present in the pyridyl ring of the INH ligand. This fact can be responsible for the orange color of the compound due to the greater electronic delocalization comprising the entire system;[34] the delocalization involves the oxocarbon ring, a region rich of delocalized electrons, arising from the two nitrogen atoms, the carbonyl groups, and the protonated pyridyl ring.

The squaraine SqINH·H_2O crystallizes in a monoclinic system with space group $P2_1$; there is a screw axis of order two along the y-axis. In Figure 2a the presence of only one water molecule per repeating unit is observed. This water molecule takes part of the N3···O9 = 2.671(3) Å hydrogen bond, classified as moderate (or medium) according to literature.[35−37] This hydrogen bond occurs through the distant interaction between the oxygen atom of the water and the protonated nitrogen atom of the pyridyl group. Note that the oxocarbon and pyridyl rings are not coplanar and there is an angle of 76.74 degrees between them; this is very important since due to this angle the entire molecule is not planar. The torsion angle among the C4−N1−N2−C5 atoms is 73.03°; whereas the average CC distance in the oxocarbon ring is 1.463(3) Å, which indicates the intermediate nature of these bonds between single and double characters.

The squaraine SqINH crystallizes in a monoclinic system with space group $P2_1/c$, with a screw axis of order two along the

dx.doi.org/10.1021/jp509502w | J. Phys. Chem. A XXXX, XXX, XXX−XXX

y-axis, glide plane [0,1,0] perpendicular with glide component [0,0,1/2] and a center of inversion. The main difference observed in SqINH (Figure 2b) relative to SqINH·H_2O is the absence of the water molecule; the absence of this specific building block causes very important structural changes, influencing the supramolecular arrangement. The planes between the oxocarbon and pyridyl rings are almost perpendicular with an angle of 89.61 degrees, and a value of 60.07° for the torsion angle among the C4−N1−N2−C5 atoms, which indicates a small rotational disturbance suffered by the system after the loss of the water molecule. The CC average distance for the oxocarbon ring is 1.4959(3) Å, a value which is close to the observed for SqINH·H_2O. It is important to note that the exit of the water molecule leaves the structure less distorted than the other, by comparing the angles of 60.07° and 73.03° for both structures; this can be understood as a spread of the electronic delocalization, which is reflected by the electronic properties for such systems. The supramolecular arrangements for both hydrated and anhydrous squaraines are shown in Figure 3. Squaraine SqINH·H_2O (Figure 3a) displays

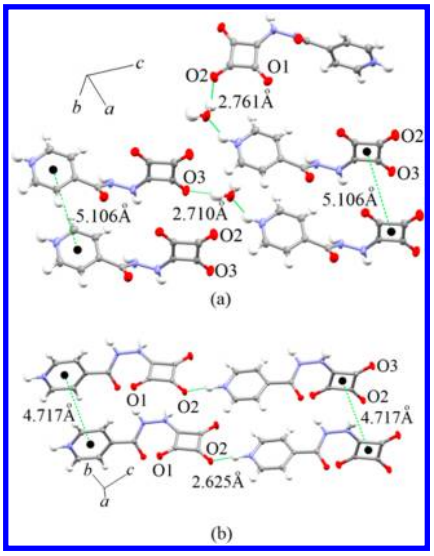

Figure 3. Supramolecular arrangements of the squaraines SqINH·H_2O (a) and SqINH (b).

a supramolecular arrangement formed by hydrogen bonds via one water molecule interacting with three different pseudo-oxocarbons groups. The bond distances are O9···O2 = 2.761(2), O9···O3 = 2.710(2), and N3···O9 = 2.671(3) Å, all of them classified as moderate.[35] There have been no observed other interactions that could also be responsible for the stability of the crystalline structure, such as C−H···π and π-stacking. It is also important to notice that the centroid−centroid distance between pyridyl−pyridyl and oxocarbon−oxocarbon groups exhibits the same value of 5.106(2) Å, which is too high to be classified as a π-stacking interaction, when compared to the reference value, around 3.800 Å.[38] Thus, it can be noticed that the loss of the water molecule, which is directly responsible for every type of interaction observed in the system, should provide a major structural change in the system in a supramolecular level.

The new supramolecular arrangement formed after the loss of the water molecule of SqINH·H_2O, due to heating, can be observed in Figure 3b. In this anhydrous structure new hydrogen bonds N3···O2 = 2.625(2) Å between the oxygen O2 atom from the oxocarbon ring and the nitrogen N3 atom from the pyridyl group can be observed. The O2 atom showed a subtle rotation, followed by a small glide of pseudo-oxocarbon promoting an approximation of the N3 atom from the protonated pyridyl group. Another important fact related to the absence of the water molecule is the approximation of the oxocarbon−oxocarbon centroids and pyridyl−pyridyl groups, at *ca.* 4.717(2) Å.

In a similar study, in which the asymmetric squaraine (2-dimethylamino-4-anilino)squaraine was investigated by spectroscopy and crystallography,[19] Silva et al. showed that their compound also crystallized in a monoclinic system, but in space group $P2_1/n$. The aniline system and the oxocarbon ring are essentially coplanar (deviation of planarity of 0.017 Å) and the CC bond distances of the oxocarbon ring are almost similar and the average is 1.452 Å, which shows a degree of electronic delocalization in the molecule.[19]

The influence of water molecules in the crystal packing, especially in the centroid−centroid approximation of the oxocarbon family, has been identified in two previous investigations in literature. Braga et al.[39] studied the influence of water molecules in different packing formed from crystalline alkali croconates; for small cations as Li^+, Na^+, and K^+, the solids usually crystallize with two water molecules per repeating unit. Meanwhile, for larger cation as Rb^+ and Cs^+, the salts are anhydrous. The water molecules are located between the planes containing the croconate ions and their loss promotes an approximation of the rings. In other words, Braga and co-workers presented a correlation between cation size and the kind of packing in the solid state. In another investigation, Da Silva et al.[40] performed a similar study involving heating potassium croconate $K_2C_5O_5·2H_2O$ salt, where it could be observed from the XRD pattern of the hydrated (orange) and anhydrous (yellow) species that the most intense peaks occurred at 2θ = 11.45 and 24.5°. These peaks represent the d_{hkl} value of 7.72 and 3.63 Å, respectively, and are indicative of a small interplanar distance for the dehydrated structure, consequently related to a possible reduction in the oxocarbon ring distance in the packing, which was also observed in the present study by single crystal diffraction. It is worth mentioning that the water withdrawing from the structure collapses the crystal structure for the potassium croconate ion, generating the loss of the crystallinity. In the present case this is not observed: the crystal can be heated, the water molecule goes out, and the crystal is still suitable for X-ray analysis.

The electronic spectrum of SqINH·H_2O solubilized in water is depicted in Figure 4. The spectrum shows an absorption band at 276 nm and a shoulder at 257 nm, which represents the same profile as the electronic spectrum of the squarate ion in water (which shows a band at 269 nm and a shoulder at 249 nm, due to the Jahn−Teller effect).[41,42] However, in the case of the squaraines, such a profile cannot be attributed to the double degeneracy effect since the substitution of the oxygen atom by the INH group generates a loss of symmetry. Despite that, the molar absorptivity coefficient of the oxocarbon group is so high that probably it overcomes the absorption generated by the other parts of the squaraine. Another fact that explains the observed profile is the intense intermolecular charge transference from the INH group to the oxocarbon ring, which can be assigned to the band at 464 nm in the water solution spectrum for SqINH. The presence of an electronic transition centered at 964 nm is very impressive; there are few works in literature about the presence of electronic transitions in that

dx.doi.org/10.1021/jp509502w | J. Phys. Chem. A XXXX, XXX, XXX−XXX

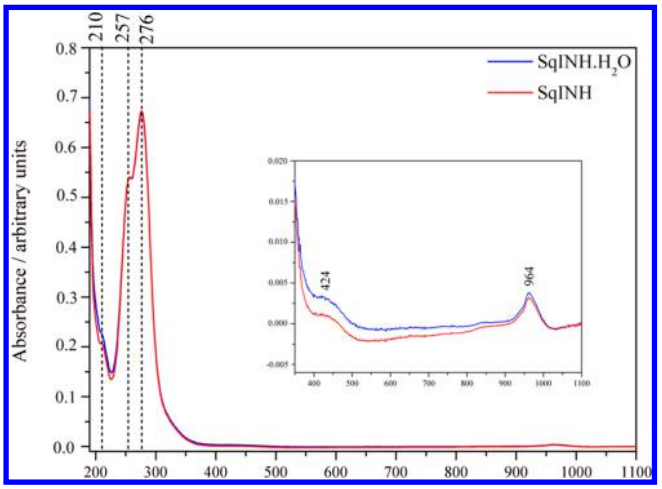

Figure 4. Electronic spectra in water of the squaraines SqINH·H_2O and SqINH.

region. Most of these works observed that for disubstituted squaraines such as quinoline-based squaraine dyes,[29] the electronic transitions in the near-infrared region of such systems, at *ca.* 700−800 nm, can be assigned to the $\pi \rightarrow \pi^*$ transition due to a better electronic delocalization over the molecule. In the present structure, the band at 964 nm can be seen as the response for the intermolecular charge transfer transition, although there is only one substituted system in the oxocarbon ring, if compared with other known squaraine dyes.[45] However, the low absorption coefficient for the electronic transition in the near-infrared can be explained by the distortion of about 60 to 70° observed in the solid state between both molecules, which prevails the effective electronic delocalization.

Two experiments were carried out in order to analyze the absorption and the fluorescence behavior of both SqINH·H_2O and SqINH squaraines in the solid state. The absorption spectra were obtained from their reflection spectra, while the fluorescence spectra were obtained from their Raman spectra excited with a green laser (532 nm), Figure 5. Although the Raman spectra of the squaraines was obtained, interest does not lie on the vibrational bands but on the spectra profile. A bare superficial comparison shows that the fluorescent emission is higher in the anhydrous compound than in the hydrated one. This fact is very interesting since the presence of the water molecule probably is responsible for the fluorescence quenching, in the case of the hydrated structure. On the other hand, the absorption presents an opposite behavior: the hydrated squaraine absorbs more radiation than the anhydrous. The bands observed in the absorption spectra (Figure 5a) are attributed to the atomic transitions from the mercury lamps of the environment, whereas all the narrow bands seen in the right spectra are due to the vibrational structures for both compounds. It is important to note the observed trend in the fluorescence emission (Figure 5b): even both systems were excited at 532 nm, the emission is centered at ca. 630 nm, which is red-shifted when compared with other similar systems described in the literature, such as the squaraine−bis-(rhodamine-6G) coordinated to several different metal ions[28] and dicyanomethylene-functionalized squaraine bound to different proteins.[43]

The IR and Raman spectra of SqINH·H_2O and SqINH are shown in Figures 6 and 7, respectively. Both squaraines show several vibrational bands in the spectra, which can be attributed to the low molecular symmetry in the solid state; the main vibrational bands of the building blocks and the derivatives, as well as a tentative assignment, based on the studies published

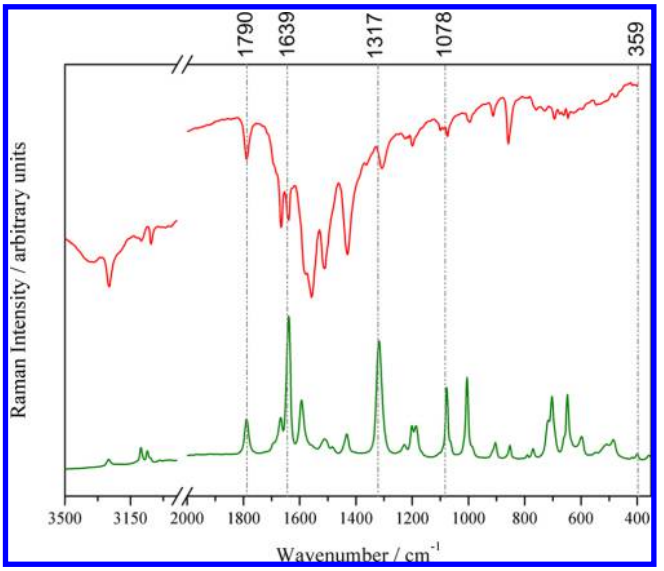

Figure 6. Infrared and Raman spectra (1064 nm) of the squaraine SqINH·H_2O.

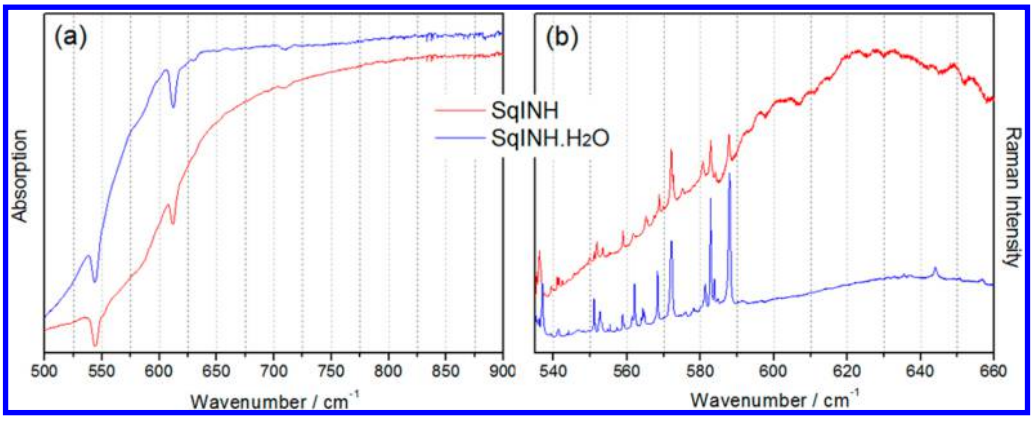

Figure 5. Absorption (a) and visible Raman (b) spectra of the squaraines SqINH·H_2O and SqINH.

dx.doi.org/10.1021/jp509502w | J. Phys. Chem. A XXXX, XXX, XXX−XXX

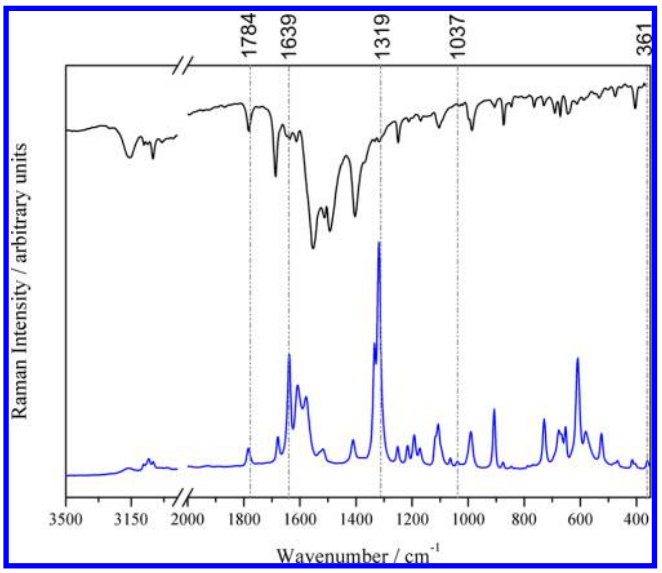

Figure 7. Infrared and Raman spectra (1064 nm) of the squaraine SqINH.

by Nakashima and Balkanski,[44] Gunasekaran et al.[20] and Akalin and Akyuz,[45] are shown in Table 4.

The vibrational spectra of both compounds corroborate with the proposition that the insertion of the INH group increases the electronic delocalization in the molecule as a whole. This can be verified mainly by the shift of the oxocarbon group bands. The Raman and IR spectra of SqINH·H_2O are presented in Figure 6. In the spectrum of the squaric acid in the solid state, the band assigned to the ν(CO) is observed at 1823 cm^{-1}, whereas for SqINH·H_2O it is shifted to 1790 cm^{-1}. The band assigned to the δ(CO) was also shifted to a lower wavenumber; it can be observed at 380 and 359 cm^{-1} for H_2Sq and SqINH·H_2O, respectively. An explanation for these shifts to lower wavenumbers is based on the force constants of the respective bonds; the bond order of the CO group has decreased in the squaraine system. It suggests lower insaturation character of the CO bond, since the electrons are less localized in this region because of the increase in the electronic conjugation.

The bands assigned to the symmetric and asymmetric stretching of the CC bonds in the oxocarbon ring were shifted to higher wavenumbers. For H_2Sq such carbon−carbon stretching modes can be observed at 1048 (symmetric CC from the oxocarbon ring) and 1617 cm^{-1} (the asymmetric C═C from the oxocarbon ring), being shifted respectively to 1078 and 1639 cm^{-1} in the squaraine. These data also corroborate with the proposition that the electronic conjugation is increasing: once the electronic density is not so concentrated near the oxygen atoms, the tendency is the increase in the force constants of the CC bonds over the oxocarbon ring.

The band at 1317 cm^{-1}, assigned to the δ(NH) mode, is strong in the Raman spectra and weak in the infrared; in the solid isoniazid spectrum this band of medium intensity is observed at 1329 cm^{-1} (see Supporting Information, Figure S3). This result corroborates with the crystallographic data: the synthetic introduction of the INH group in the oxocarbon ring

Table 4. Tentative Vibrational Assignment of the Main Bands of the Precursors and the Synthesized Squaraines (in cm^{-1})[20,45]

H_2Sq	INH		SqINH·H_2O		SqINH		
Raman	IR	Raman	IR	Raman	IR	Raman	tentative assignment
	3304 (m)	3309 (vw)	3265 (w)	3267 (vw)	3155 (w)	3159 (vw)	ν_s(NH)
	3111 (m)	3114 (w)					ν_s(NH_2)
		3072 (m)		3093(w)	3082 (vw)	3084 (vw)	ν_{as}(CH) of INH
	3051 (vw)	3060 (w)		3060 (w)	3061 (vw)	3057 (w)	ν_{as}(CH) of INH
	3015 (vw)	3033 (vw)	3040 (w)	3045 (vw)	3034 (w)	3031 (vw)	ν_{as}(CH) of INH
1823 (vw)			1786 (w)	1790 (m)	1782 (w)	1784 (w)	ν(CO) squarate ring
	1669 (vs)	1676 (m)	1666 (m)	1668 (m)	1686 (m)	1678 (w)	ν(CO) of INH
1617 (w)			1643 (w)	1639 (vs)	1635 (vw)	1639 (s)	ν_{as}(CC) squarate ring
	1603 (m)	1608 (vs)	1587 (w)	1593 (m)	1612 (vw)	1608 (s)	ν_{as}(CC) of py ring
	1556 (vs)	1558 (w)	1558 (s)		1553 (vs)	1577 (s)	ν_s(CN) of py ring
	1493 (m)	1500 (vw)	1514 (m)	1512 (w)	1512 (w)	1517 (w)	δ(H−N−N)
	1412 (s)	1417 (vw)	1433 (m)	1433 (w)	1404 (m)	1410 (w)	ν_s(CC) of py ring
	1335 (s)	1338 (s)			1333 (vw)	1334 (s)	ν(CN) of INH
		1329 (m)	1315 (vw)	1317 (vs)	1317 (vw)	1319 (vs)	δ(NH)
			1246 (vw)		1250 (w)	1252 (w)	ν(CC) of py ring
	1221 (s)	1225 (s)	1223 (vw)	1228 (vw)	1211 (vw)	1216 (w)	δ(CH) of INH + ν(CC) of py ring
	1192 (vw)	1193 (s)	1200 (w)	1201 (m)	1200 (vw)	1192 (w)	ν(NN) + ν(CN) + δ(CH) + ν(CC) of py ring
	1142 (s)	1138 (w)			1132 (vw)	1037 (vw)	δ(CH) + ν(CC) py + ν(CN)
	1097 (vw)	1101 (w)	1101 (vw)		1103 (m)	1107 (m)	ν(CN) py + δ(CH) + ν(CN)
1048 (w)			1076 (w)	1078 (s)	1031 (vw)	1037 (vw)	ν(CC)
	995 (vs)	1010 (vs)	1003 (vw)	1005 (s)	986 (w)	991 (m)	ν(CC) py + δ(CC) py
	889 (m)	895 (m)	912 (w)	904 (w)	905 (vw)	906 (w)	ω(CH) + ω(C−NH_2)
	845 (s)	856 (w)	858 (w)	852 (w)	874 (w)	875(mw)	ω(CH) + ω(C−NH_2)
726 (vs)			710 (vw)	704 (s)	729 (w)	728 (m)	Squaric ring breath
	675 (s)	673 (m)	634 (vw)	648 (s)	690 (w)	677 (m)	δ(C−C═O)
635 (s)				598 (w)	611 (w)	609 (s)	δ of squaric ring
	505 (m)	511 (w)		507 (w)	532 (w)	524 (w)	ω(HNNH) + ω(NH) + δ(NCC) + δ(C−NH_2) + δ(OCC)
380 (s)				359 (vw)		361 (vw)	δ(CO)

dx.doi.org/10.1021/jp509502w | J. Phys. Chem. A XXXX, XXX, XXX−XXX

occurs by the nitrogen atom from the $-NH_2$. Similar analysis could have been done based on the bands related to the vibrational modes of the INH group. However, since this group is rather complex, no linearity was observed in the band shifts. Nevertheless, through the squarate group bands, it was possible to infer the behavior of the INH group, which means that the oxocarbon group assumed the role of a spectroscopic probe.

The vibrational data of the SqINH squaraine also show an increase in its electronic delocalization compared with that of the precursors and the hydrated squaraine. The Raman and IR spectra are presented in Figure 7. The bands assigned to the ν(CO) and δ(CO) modes were also shifted to lower wavenumbers (1784 and 361 cm^{-1}, respectively). The band at 1037 cm^{-1}, assigned to ν(CC) mode, remained approximately unchanged; the band at 1639 cm^{-1}, attributed to ν_{ass}(CC), was also shifted to a lower wavenumber, as observed for the hydrated squaraine. As in the SqINH·H_2O spectrum, a band strongly intense in the Raman and weak in the infrared spectrum at 1319 cm^{-1} was observed and assigned to the δ(NH) mode; the shift of this band, specially, shows that the bond interaction between INH and the squarate ring occurs by the nitrogen atom of the $-NH_2$ group.

All these results show that the synthesized squaraines possess a higher level of electronic delocalization when compared with the precursor squaric acid. The crystallographic, electronic, and vibrational data indicate the extension of the electronic delocalization all over both the molecules structures, and the presence of the water molecule is a factor of quenching for fluorescence, since the emission spectra for both compounds clearly shows the decrease of fluorescence when water the molecule is present. Clearly this squaraine does not have the same solid state properties such as the ones with double substituents, but the effect of the electronic delocalization over the molecule, even the one containing the water molecule, is highly related to the intramolecular electronic transition observed for both structures, evidenced by the reported electronic absorption and emission data.

CONCLUSIONS

In this study we have reported the synthesis and the results of spectroscopic (Raman, IR, and electronic) and structural investigations of the squaraine SqINH·H_2O and its respective anhydrous compound SqINH. The hydrated squaraine possesses one water molecule per repeating unit in its structure. Both squaraines crystallize in the monoclinic system, but with different space groups. The SqINH·H_2O belongs to the $P2_1$ group, while the SqINH belongs to the $P2_1/c$ group. The crystallographic data show that the loss of the water molecule generates great changes in the supramolecular interactions, altering the hydrogen bonds and centroid−centroid distances.

One feature in common for the two of them is the π-system conjugation through the entire molecule. It is grounded on the fact that the length of several bonds in the system presents average values between single and double bonds. Furthermore, the vibrational and electronic bands shifts referred to the oxocarbon group confirm this electronic delocalization expansion. Moreover, the presence of the water molecule is responsible for diminishing the fluorescence, since comparison between the two emission spectra clearly shows the dehydrated squaraine is a better fluorescence emission system than the hydrated squaraine.

ASSOCIATED CONTENT

Supporting Information

Thermogravimetric curves (TGA and DTA) for both derivatives and Raman spectrum of isoniazid at 1064 nm excitation. This material is available free of charge via the Internet at http://pubs.acs.org.

AUTHOR INFORMATION

Corresponding Author

*E-mail: luiz.oliveira@ufjf.edu.br. Tel.: +55 (32) 3229-3310. Fax: +55 (32) 3229-3310.

Notes

The authors declare no competing financial interest.

ACKNOWLEDGMENTS

The authors thank CNPq, FAPEMIG, CAPES, and FINEP for financial support and also LabCri (Departamento de Física, UFMG) for the X-ray facilities.

REFERENCES

(1) de Oliveira, V. E.; Diniz, R.; de Oliveira, L. F. C. Oxocarbons, Pseudo-Oxocarbons and Squaraines. *Quim. Nova* **2009**, *32*, 1917−1925.

(2) West, R. Chemistry of the Oxocarbons. *Isr. J. Chem.* **1980**, *20*, 300−307.

(3) de Oliveira, L. F. C.; Gonçalves, N. S.; Santos, P. S.; Muterelli, S. R. Structure and Vibrational Spectroscopy of Oxocarbonos and Its Coordination Species. *Quim. Nova* **1992**, *15*, 55−61.

(4) de Oliveira, L. F. C.; Santos, P. S. The Interaction of The Squarate Ion with Trivalent Transition Metal Ions as Revealed by Resonance Raman Spectroscopy. *J. Mol. Struct.* **1992**, *269*, 85−96.

(5) de Oliveira, V. E.; Diniz, R.; de Oliveira, L. F. C. Oxocarbons, Pseudo-Oxocarbons and Squaraines. *Quim. Nova* **2009**, *32*, 1917−1925.

(6) Fatiadi, A. J. Oxocarbons and Pseudo-oxocarbons. 10. Pseudo-oxocarbons—Synthesis of 2,1,3-Bis-(Dicyanomethylene) and 1,2,3-Tris-(Dicyanomethylene) Croconate Salt—New Bond-Delocalized Dianions, Croconate Violet and Croconate Blue. *J. Res. Natl. Bur. Stand.* **1980**, *85*, 73−86.

(7) de Oliveira, V. E.; de Carvalho, G. S.; Yoshida, M. I.; Donnici, C. L.; Speziali, N. L.; Diniz, R.; de Oliveira, L. F. C. Bis-(dicyanomethylene)squarate Squaraines in Their 1,2- and 1,3-Forms: Synthesis, Crystal Structure and Spectroscopic Study of Compounds Containing Alkali Metals and Tetrabutylammonium Ions. *J. Mol. Struct.* **2009**, *936*, 239−249.

(8) Radaram, B.; Mako, T.; Levine, M. Sensitive and Selective Detection of Cesium via Fluorescence Quenching. *Dalton Trans.* **2013**, *42*, 16276−16278.

(9) Huang, Y.; Lin, Q.; Wu, J.; Fu, N. Design and Synthesis of a Squaraine Based Near-Infrared Fluorescent Probe for the Ratiometric Detection Of Zn^{2+} Ions. *Dyes Pigm.* **2013**, *99*, 699−704.

(10) Ananda Rao, B.; Kim, H.; Son, Y.-A. Synthesis of Near-Infrared Absorbing Pyrylium-Squaraine Dye for Selective Detection of Hg^{2+}. *Sens. Actuators B* **2013**, *188*, 847−856.

(11) Ramaiah, D.; Eckert, I.; Arun, K. T.; Weidenfeller, L.; Epe, B. Squaraine Dyes for Photodynamic Therapy: Study of Their Cytotoxicity and Genotoxicity in Bacteria and Mammalian Cells. *Photochem. Photobiol.* **2002**, *76*, 672−677.

(12) Gräf, K.; Rahim, M. A.; Das, S.; Thelakkat, M. Complementary Co-Sensitization of an Aggregating Squaraine Dye in Solid-State Dye-Sensitized Solar Cells. *Dyes Pigm.* **2013**, *99*, 1101−1106.

(13) Cicero, G.; Musso, G.; Lamberti, A.; Camino, B.; Bianco, S.; Pugliese, D.; Risplendi, F.; Sacco, A.; Shahzad, N.; Ferrari, A. M.; Ballarin, B.; Barolo, C.; Tresso, E.; Caputo, G. Combined Experimental and Theoretical Investigation of the Hemi-squaraine/

TiO_2 Interface for Dye Sensitized Solar Cells. *Phys. Chem. Chem. Phys.* **2013**, *15*, 7198−7203.
(14) Gao, F.-P.; Lin, Y.-X.; Li, L.-L.; Liu, Y.; Mayerhöffer, U.; Spenst, P.; Su, J.-G.; Li, J.-Y.; Würthner, F.; Wang, H. Supramolecular Adducts of Squaraine and Protein for Noninvasive Tumor Imagingand Photothermal Therapy in Vivo. *Biomaterials* **2014**, *35*, 1004−1014.
(15) Liu, X.-D.; Sun, R.; Ge, J.-F.; Xu, Y.-J.; Xu, Y.; Lu, J.-M. A Squaraine-Based Red Emission Off−On Chemosensor for Biothiols and Its Application in Living Cells Imaging. *Org. Biomol. Chem.* **2013**, *11*, 4258−4264.
(16) Sreejith, S.; Carol, P.; Chithra, P.; Ajayaghosh, A. Squaraine Dyes: A Mine of Molecular Materials. *J. Mater. Chem.* **2008**, *18*, 264−274.
(17) de Oliveira, V. E.; Freitas, M. C. R.; Diniz, R.; Yoshida, M. I.; Speziali, N. L.; Edwards, H. G. M.; de Oliveira, L. F. C. Crystal Structure and Vibrational Spectra of Some Metal Complexes of Pseudo-Oxocarbon Bis(dicyanomethylene)squarate in Its Cis and Trans Forms. *J. Mol. Struct.* **2008**, *881*, 57−67.
(18) Ribeiro, M. C. C.; de Oliveira, L. F. C.; Santos, P. S. Raman Bandshape Analysis of Oxocarbon Ions in Aqueous Solutions. *Chem. Phys.* **1997**, *217*, 71−81.
(19) Silva, C. E.; Diniz, R.; Rodrigues, B. L.; de Oliveira, L. F. C. Crystal Structure and Spectroscopic Analysis of the Asymmetric Squaraine [(2-Dimethylamino-4-anilino)squaraine]. *J. Mol. Struct.* **2007**, *831*, 187−194.
(20) Gunasekaran, S.; Sailatha, E.; Seshadri, S.; Kumaresan, S. FTIR, FT Raman Spectra and Molecular Structural Confirmation of Isoniazid. *Indian J. Pure Appl. Phys.* **2009**, *47*, 12−18.
(21) Gadad, A. K.; Noolvi, M. N.; Karpoormath, R. V. Synthesis and Anti-tubercular Activity of a Series of 2-Sulfonamido/Trifluoromethyl-6-Substituted Imidazo[2,1-b]-1,3,4-thiadiazole Derivatives. *Bioorgan. Med. Chem.* **2004**, *12*, 5651−5659.
(22) Karimi, M. A.; Mazloum-Ardakani, M.; Mashhadizadeh, M. H.; Banifatemeh, F. Simultaneous Kinetic Spectrophotometric Determination of Hydrazine and Isoniazid Using H-Point Standard Addition Method and Partial Least Squares Regression in Micellar Media. *Croat. Chem. Acta* **2009**, *82*, 729−738.
(23) Naik, R. M.; Prasad, S.; Kumar, B.; Yadav, S. B. S.; Asthana, A.; Yoshida, M. Ligand Substitution Kinetic Assay of Antitubercular Drug Isoniazid in Pure and Pharmaceutical Formulations. *Microchem. J.* **2013**, *111*, 108−115.
(24) Sinha, N.; Jain, S.; Tilekar, A.; Upadhayaya, R. S.; Kishore, N.; Jana, G. H.; Arora, S. K. Synthesis of Isonicotinic Acid *N*′-Arylidene-*N*-[2-oxo-2-(4-aryl-piperazin-1-yl)-ethyl]-hydrazides as Antituberculosis Agents. *Bioorg. Med. Chem. Lett.* **2005**, *15*, 1573−1576.
(25) Imramovský, A.; Polanc, S.; Vinšová, J.; Kočevar, M.; Jampílek, J.; Rečková, Z.; Kaustová, J. A New Modification of Anti-tubercular Active Molecules. *Bioorgan. Med. Chem.* **2007**, *15*, 2551−2559.
(26) Shingnapurkar, D.; Dandawate, P.; Anson, C. E.; Powell, A. K.; Afrasiabi, Z.; Sinn, E.; Pandit, S.; Venkateswara Swamy, K.; Franzblau, S.; Padhye, S. Synthesis and Characterization of Pyruvate−Isoniazid Analogs and Their Copper Complexes as Potential ICL Inhibitors. *Bioorg. Med. Chem. Lett.* **2012**, *22*, 3172−3176.
(27) Yan, Z.; Guang, S.; Su, X.; Xu, H. Near-Infrared Absorbing Squaraine Dyes for Solar Cells: Relationship between Architecture and Performance. *J. Phys. Chem. C* **2012**, *116*, 8894−8900.
(28) So, H.-S.; Rao, B. A.; Hwang, J.; Yesudas, K.; Son, Y.-A. Synthesis of Novel Squaraine−bis(rhodamine-6G): A Fluorescent Chemosensor for the Selective Detection of Hg^{2+}. *Sensor Actuat. B* **2014**, *202*, 779−787.
(29) *RED C*, 1.171.32.38 ed.; Oxford Diffraction Ltd.: Abingdon, England, 2008.
(30) Larson, A. C. *Int. Union Crystall. Symp.* **1969**, 291−294.
(31) Blessing, R. H. An Empirical Correction for Absorption Anisotropy. *Acta Crystallogr. A* **1995**, *51*, 33−38.
(32) Farrugia, L. J. ORTEP-3 for Windows—A version of ORTEP-III with a Graphical User Interface (GUI). *J. Appl. Crystallogr.* **1997**, *30*, 565−565.
(33) Macrae, C. F.; Edgington, P. R.; McCabe, P.; Pidcock, E.; Shields, G. P.; Taylor, R.; Towler, M.; van de Streek, J. Mercury: Visualization and Analysis of Crystal Structures. *J. Appl. Crystallogr.* **2006**, *39*, 453−457.
(34) de Oliveira, V. E.; Freitas, M. C. R.; Diniz, R.; Yoshida, M. I.; Speziall, N. L.; Edwards, H. G. M.; de Oliveira, L. F. C. Crystal Structure and Vibrational Spectra of Some Metal Complexes of Pseudo-oxocarbon Bis(Dicyanomethylene)Squarate in Its Cis and Trans Forms. *J. Mol. Struct.* **2008**, *881*, 57−67.
(35) Garcia, H. C.; Cunha, R. T.; Diniz, R.; de Oliveira, L. F. C. Co-crystal and Crystal: Supramolecular Arrangement Obtained from 4-Aminosalicylic Acid, BPA Ligand and Cobalt Ion. *J. Mol. Struct.* **2012**, *1010*, 104−110.
(36) Georgopoulos, S. L.; Diniz, R.; Rodrigues, B. L.; de Oliveira, L. F. C. Crystal Structure and Raman Spectra of Rubidium Hydrogen Squarate. *J. Mol. Struct.* **2005**, *741*, 61−66.
(37) Lopes, J. G. S.; de Oliveira, L. F. C.; Edwards, H. G. M.; Santos, P. S. The Raman Spectrum of Thiourea−Oxocarbon Adducts. *J. Raman Spectrosc.* **2004**, *35*, 131−139.
(38) Khlobystov, A. N.; Blake, A. J.; Champness, N. R.; Lemenovskii, D. A.; Majouga, A. G.; Zyk, N. V.; Schröder, M. Supramolecular Design of One-Dimensional Coordination Polymers Based on Silver(I) Complexes of Aromatic Nitrogen-Donor Ligands. *Coord. Chem. Rev.* **2001**, *222*, 155−192.
(39) Braga, D.; Maini, L.; Grepioni, F. Croconic Acid and Alkali Metal Croconate Salts: Some New Insights Into an Old Story. *Chem.—Eur. J.* **2002**, *8*, 1804−1812.
(40) da Silva, C. E.; Garcia, H. C.; Diniz, R.; Spezialli, N. L.; Yoshida, M. I.; Edwards, H. G.; de Oliveira, L. F. New Insight on The Investigation of The Role of Water in the Solid-State Structures of Potassium Croconate, $K_2C_5O_5.2H_2O$, and Its Anhydrate. *J. Phys. Chem. A* **2007**, *111*, 11990−11995.
(41) Hjima, M.; Udagawa, Y.; Kaya, K.; Ito, M. RamanSpectra and Jahn-Teller Effects of $C_4O_4^{2-}$ and $C_5O_5^{2-}$ Ions. *Chem. Phys.* **1975**, *9*, 229−235.
(42) de Oliveira, L. F. C.; Santos, P. S. Chromophore Selective Resonance Raman Enhancement in Copper(II) Squarate Complexes with Nitrogenous Counterligands. *J. Mol. Struct.* **1991**, *245*, 215−220.
(43) Jin, B.; Zhang, X.; Zheng, W.; Liu, X.; Zhou, J.; Zhang, N.; Wang, F.; Shangguan, D. Dicyanomethylene-Functionalized Squaraine as a Highly Selective Probe for Parallel G-Quadruplexes. *Anal. Chem.* **2014**, *86*, 7063−7070.
(44) Nakashima, S.; Balkanski, M. Raman Study of Squaric Acid. *Solid State Commun.* **1976**, *19*, 1225−1228.
(45) Akalin, E.; Akyuz, S. Vibrational Structure of Free and Hydrogen Bonded Complexes of Isoniazid: FT-IR, FT-Raman and DFT Study. *J. Mol. Struct.* **2007**, *834−836*, 492−497.